An *LC*-Type Passive Wireless Humidity Sensor System With Portable Telemetry Unit

Cong Zhang, Li-Feng Wang, *Member, IEEE*, Jian-Qiu Huang, *Member, IEEE*, and Qing-An Huang, *Senior Member, IEEE*

***Abstract*— This paper presents a high-sensitivity passive wireless humidity sensor system with a portable telemetry unit for applications in sealed environments. A complementary metal oxide semiconductor (CMOS) interdigital capacitive humidity sensor die was attached to an organic substrate (FR-4) on which a fixed planar spiral copper inductor was fabricated. The variable capacitor and the fixed inductor were wire bonded to form an inductor–capacitor (*LC*) tank circuit. The resonant frequency of the sensor tank is dependent on the sensor capacitance, which changes in response to the humidity. The sensitivity of the capacitive sensor was improved significantly using graphene oxide as a sensing material. The package-level integration was achieved by employing the embedded inductor on an organic packaging substrate. The *LC*-type sensor is interrogated wirelessly using our homemade portable telemetry unit, which is based on a standing wave ratio bridge to measure the real part of the readout coil impedance. Measurements show a sensitivity of −18.75 kHz/%RH over a range of 15%–95% RH. The implemented telemetry unit addresses the need for a low-cost, portable, and universal reader of the *LC*-type passive wireless sensors. [2013-0188]**

***Index Terms*— Humidity sensor, LC resonant sensor, passive sensor, wireless sensor, telemetry.**

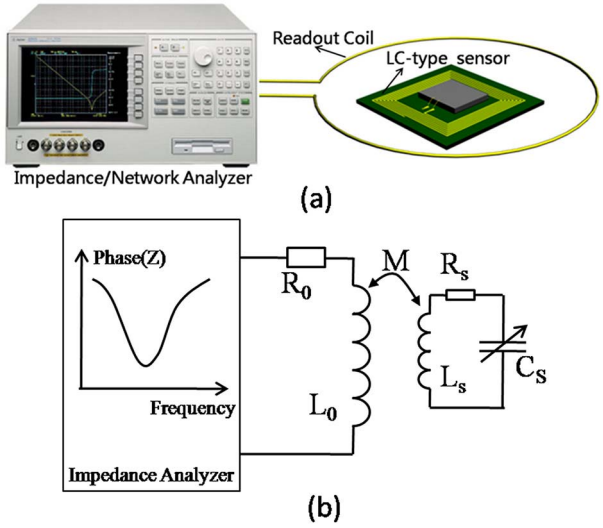

Fig. 1. LC-type passive wireless sensing system. (a) Schematic diagram. (b) Equivalent circuit.

I. Introduction

LC-TYPE PASSIVE wireless sensors have been developed to monitor various parameters of interest in situations where wired connections are difficult or even impossible, such as pressure [1]–[3], strain [4], temperature [5], threshold g-value [6], pH [7]. This non-contact measurement technique utilizes an LC resonant tank to determine the parameters of interest remotely. The sensing principle is usually based on changes of the capacitance, inductance or both of them which represent a variation on the resonant frequency of the sensor tank [8]. A schematic diagram and an equivalent circuit of an LC-type passive wireless sensing system are shown in Fig. 1, where the sensor element consists of a fixed inductor and a variable capacitor. To wirelessly interrogate the LC-type sensor, an external readout coil is magnetically coupled to the sensor and the resonant frequency of the sensor tank is determined through the readout coil impedance.

Despite the obvious advantages, such as simplicity, low power dissipation, and non-contact interrogation, the main problem of the LC-type passive wireless sensors remains the wireless readout [9]. Most researches about the LC-type passive wireless sensors focused on the design of sensing elements for all kinds of applications and then a so-called phase-dip technique was often applied to wirelessly determine the resonant frequency of the sensor tank using a commercial impedance/network analyzer [10]. In order to avoid the need of expensive, bulky commercial instruments in practical applications, a portable custom-made reader is required [11]. Additionally, the phase-dip frequency is related to the inductive coupling coefficient, thus requiring some additional compensation methods [12].

Humidity sensors are of great importance and have been widely applied in the fields of meteorology, industry control and medical instrument. There have been lots of researches on various types of humidity sensors [13]–[15]. However, it is challengeable to utilize these sensors to monitor humidity in sealed environments, such as food packages and constructions, where a physical connection between the sensor and the reader is often difficult, or in some cases even impossible. So, remote sensing techniques are required, of which LC-type

Manuscript received June 12, 2013; revised June 20, 2014; accepted June 25, 2014. Date of publication October 2, 2014; date of current version June 1, 2015. This work was supported in part by the National Natural Science Foundation of China under Grant 61136006, and in part by the National High Technology Research and Development Program of China under Grant 2013AA041101. Subject Editor H. Seidel.

The authors are with the Key Laboratory of MEMS of the Ministry of Education, Southeast University, Nanjing 210096, China (e-mail: hqa@seu.edu.cn).

Color versions of one or more of the figures in this paper are available online at http://ieeexplore.ieee.org.

Digital Object Identifier 10.1109/JMEMS.2014.2333747

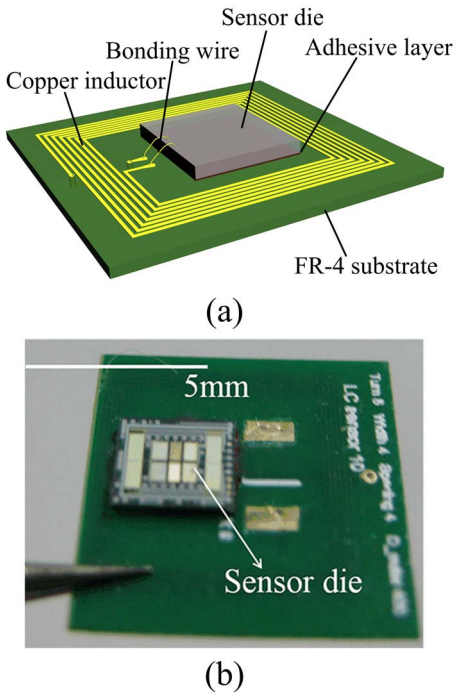

Fig. 2. LC-type passive wireless humidity sensor. (a) Schematic view. (b) Optical image.

passive wireless sensing technique enables long-term monitoring without battery lifetime issues. Wireless measurement of humidity in sealed environment was reported using a passive LC resonant tank consisting of a capacitive humidity sensor chip with ultrathin polyimide films and a hybrid coil [16]. It has been demonstrated by our group that the sensitivity of capacitive humidity sensor can be improved significantly by using graphene oxide films rather than polyimide as sensing material [17].

In this paper, we present a high-sensitivity LC-type passive wireless humidity sensor based on graphene oxide. The sensor consists of a complementary metal oxide semiconductor (CMOS) interdigital capacitive humidity sensor die and a fixed planar spiral copper inductor on a FR-4 substrate. Also, a portable telemetry unit is implemented for the LC-type passive wireless sensors, which measures the real part of the readout coil impedance rather than the phase like the normal phase-dip technique, thus eliminating the need for coupling coefficient compensation. At last, the LC-type passive wireless humidity sensors are characterized by using our homemade portable telemetry unit.

II. Sensor Element

The passive humidity sensor is a parallel-connected LC tank circuit, which consists of a CMOS interdigital capacitive humidity sensor die and a fixed planar spiral copper inductor on a FR-4 substrate, as shown in Fig. 2. The resonant frequency of the sensor tank is dependent on the sensor capacitance, which changes in response to the humidity.

The basic structure of the capacitive sensor without sensing material is an Al interdigital capacitor on silicon substrate, which is fabricated by a standard CMOS fabrication process.

TABLE I
Comparison Between Excepted Resonant Frequency and Measured One

Theoretical Inductance (Modified Wheeler Formula)	0.526 μH
Measured Self-resonant Frequency	242.5 MHz
Calculated parasitic capacitance	0.82 pF
Measured Sensor Capacitance*	31.8 pF
Calculated Resonant Frequency	38.42 MHz
Measured Resonant Frequency+	36.2 MHz

*The capacitors are directly measured by using a LCR meter at 100 kHz, 25□C, and 55% RH.
+The measured resonant frequencies listed above are also at the same temperature and relative humidity.

After dicing, the individual sensor die is attached to a FR-4 substrate with an adhesive layer. A planar spiral copper inductor (thickness=18 μm, turn=5, space=width=4 mil, outer diameter=400 mil) is first realized directly on the same FR-4 substrate by using the standard PCB process. Then, the electrical connection between the capacitor and the inductor on the substrate is made by wire bonding. At last, graphene oxide dispersion is dripped on the sensing area of the sensor chip, which is then baked for 2 hours at 50°C.

The inductance of the planar copper inductor is calculated by the well-known modified Wheeler formula, which is shown as [18]

$$L = K_1 \mu_0 \frac{n^2 d_{avg}}{1 + K_2 \delta} \tag{1}$$

$$d_{avg} = \frac{d_{out} + d_{in}}{2} \tag{2}$$

$$\delta = \frac{d_{out} - d_{in}}{d_{out} + d_{in}} \tag{3}$$

where μ_0 is the magnetic permeability of free space, n is the number of turns, d_{out} is the outer diameter, d_{in} is the inner diameter, d_{avg} is the average diameter. K_1, K_2 are both layout dependent and are 2.34, 2.75 respectively for planar square inductors. δ is the fill ratio, representing how hollow the inductor is. Thus, the calculated inductance is 0.526 μH. Here, the modified Wheeler formula is used to confine the resonant frequency of the sensor tank to locate in frequency band of our custom made reader.

In order to get the expected resonant frequency, the parasitic capacitance of the planar inductor and the sensor capacitance should be evaluated. The parasitic capacitance may be estimated by measuring the self-resonant frequency of the planar inductor. The measured self-resonant frequency by using an Agilent HP8719ES network analyzer is about 242.5MHz. Thus, calculated parasitic capacitance is about 0.82pF.

The sensor capacitor disconnected with planar inductor has been directly measured by using a LCR meter (YD-2810B)

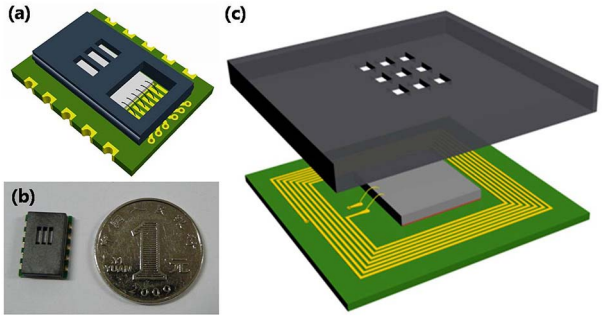

Fig. 3. (a) Leadless package for wired humidity sensor. (b) Actual package for wired humidity sensor. (c) Schematic view of the LC-type passive wireless humidity sensor package.

and the measured capacitance (at 10 kHz, 25°C, and 55%RH) is 31.8pF. Thus, the expected resonant frequency is about 38.38MHz. These results have been listed in Table I for comparison with the measured resonant frequency.

Planar spiral embedded inductors on organic packaging substrates are employed for two advantages. Firstly, high-Q, micro-henry inductors can be easily fabricated using the standard PCB process. LC-type passive wireless sensors typically operate at resonance in the low frequency domain, which necessitates the use of large inductance value. Quality factor of the inductor also should be optimized to maximize the sensitivity and the operation distance. Secondly, the package-level integration is achieved by employing the embedded inductors. In our previous work, a package for the wired humidity sensor has been reported [19], [20], as shown in Fig. 3(a) and (b). The package can be suitable for the proposed LC-type passive wireless humidity sensor when only a minor modification is carried out, that is the pattern etched onto the copper film on the FR-4 substrate should be changed to a planar inductor, as shown in Fig. 3(c).

III. Telemetry System

The wireless determination of the resonant frequency of the LC-type sensors can be done both with time and frequency domain measurement techniques [21]. As shown in Fig. 4, in time domain measurement the reader first energizes the sensor tank during a transmit phase and then records the ring down response of the sensor tank during the receive phase, which is a damped oscillation at its natural resonant frequency [22]. Sensor signal sample must be collected within tens of nanoseconds of transmit bust, due to rapid decay. Although the time domain measurement could allow a higher detection distance due to its more flexible power supply, it is not widely used in most researches because of its lower frequency resolution and the high difficulty of the implementation.

On the other hand, the frequency domain measurement allows a higher frequency resolution but a shorter maximum sensor detection distance, but it is sufficient for many special applications. For practical applications the readout system must be low-cost and portable, eliminating the need for a bulky and expensive impedance/network analyzer.

This paper presents a novel method for wirelessly interrogating LC-type sensor in frequency domain, which is based on a SWR bridge. In this section, an analytical model is first studied, which is based on a loosely coupled transformer. Then, the readout circuit is proposed, which measures the real part of the readout coil impedance to determine the resonant frequency.

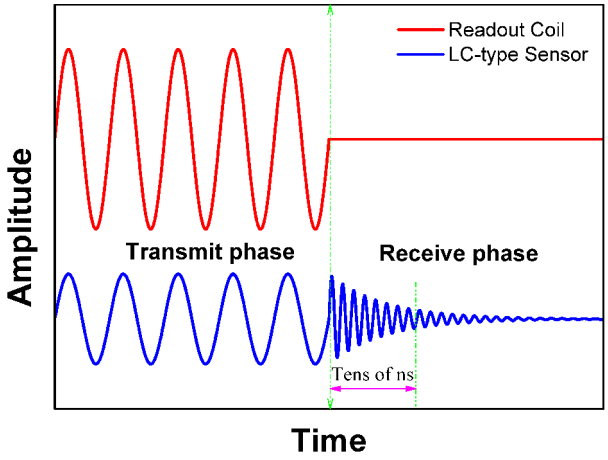

Fig. 4. Energizing signal and sensor response in time domain measurement. During the transmit phase, the sensor reacts at the same frequency as it gathers energy. When the excitation is removed, the sensor tank produces a damped oscillation at its natural resonant frequency.

A. Analytical Model

The concept for the LC-type passive wireless humidity sensor implements an LC resonant tank with humidity-sensitive capacitance to inductively couple with an external readout coil. Through inductive coupling, the external readout coil energizes the sensor tank circuit and the impedance of the sensor tank is reflected back to the external coil, as shown in Fig. 5(a).

Reflected impedance denoted with Z_T is given by

$$Z_T = \frac{\omega^2 M^2}{R_s + j\omega L_S - j\frac{1}{\omega C_S}} \tag{4}$$

where L_S, C_S, and R_s are the inductance, capacitance, and resistance of the sensor tank, respectively, and M is the mutual inductance of the two inductors.

Equivalent input impedance (Z_{in}) of the readout coil can be represented by

$$Z_{in} = R_0 + j\omega L_0 + \frac{\omega^2 M^2}{R_s + j\omega L_S - j\frac{1}{\omega C_S}} \tag{5}$$

Using the following substitutions

$$f_s = \frac{1}{2\pi\sqrt{L_S C_S}} \tag{6}$$

$$Q = \frac{1}{R_S}\sqrt{\frac{L_S}{C_S}} \tag{7}$$

$$M = k\sqrt{L_0 L_S} \tag{8}$$

where f_s and Q are the resonant frequency and the quality factor of the sensor tank, respectively, and k is the coupling coefficient between the two inductors, Z_{in} can be rewritten and

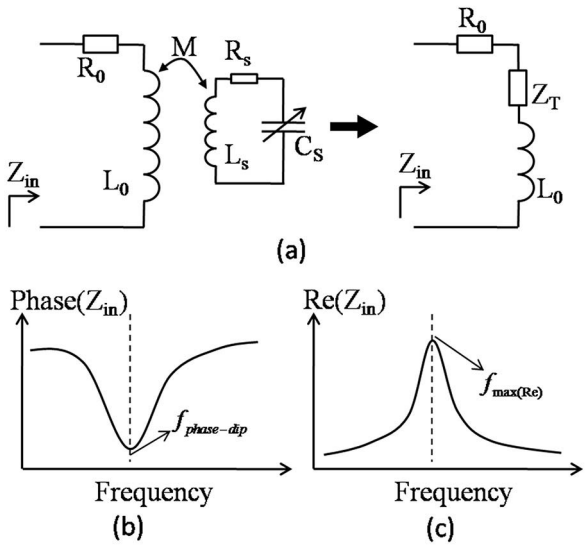

Fig. 5. (a) Equivalent input impedance of the readout coil. (b) Impedance phase versus frequency. (c) Impedance real part versus frequency.

then the real part ($Re\,(Z_{in})$), the imaginary part ($Im\,(Z_{in})$) and the phase ($\angle Z_{in}$) of Z_{in} can be expressed as

$$Im\,(Z_{in}) = 2\pi f L_0 \left[1 + k^2 Q^2 \frac{1-\left(\frac{f}{f_S}\right)^2}{1+Q^2\left(\frac{f}{f_S}-\frac{f_S}{f}\right)^2}\right] \quad (9)$$

$$Re\,(Z_{in}) = R_0 + 2\pi L_0 k^2 Q \frac{f\frac{f}{f_S}}{1+Q^2\left(\frac{f}{f_S}-\frac{f_S}{f}\right)^2} \quad (10)$$

$$\angle Z_{in} = arctan\frac{Im\,(Z_{in})}{Re\,(Z_{in})} \quad (11)$$

In most reported works, the non-contact detection of the resonant frequency of the LC-type passive wireless sensor is achieved through the phase-dip technique as the phase of the complex impedance of the readout coil drops to the minimum at a frequency near the resonant frequency, as shown in Fig. 5(b). However, the exact phase-dip frequency($f_{phase-dip}$) is determined not only by the resonant frequency of the sensor tank (f_S), but also by the coupling coefficient. Through the derivative of the frequency it can be expressed as

$$f_{phase-dip} = \left[f_S \Big/ \sqrt{2Q^2\left(1-k^2\right)}\right] \sqrt{k^2Q^2+1-2Q^2+\sqrt{\left(k^2Q^2+1-2Q^2\right)^2+12Q^4\left(1-k^2\right)}} \quad (12)$$

which can be simplified by taking the Taylor series expansion as

$$f_{phase-dip} \approx \left(1+\frac{1}{4}k^2+\frac{1}{8Q^2}\right) f_S \quad (13)$$

where the coupling coefficient k is totally dependent of physical geometries of the two inductors and also the separation distance between them. So some methods should be taken to compensate the error caused by the varying coupling coefficient.

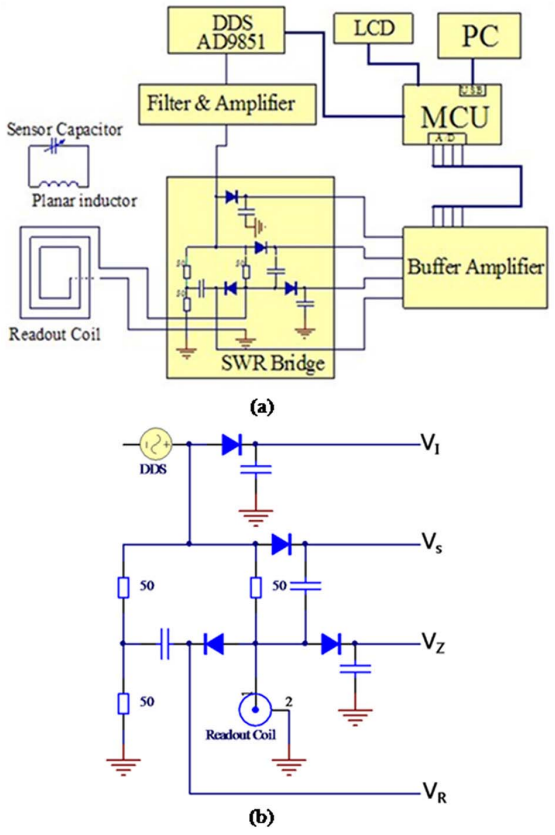

Fig. 6. (a) Schematic of the portable telemetry unit. (b) Four measured voltages of the SWR bridge.

In fact, the impedance real part $Re(Z_{in})$ is also a well-suited quantity to determine the resonant frequency of the sensor tank [22]. As shown in Fig. 5(c), the resonant frequency can be obtained from the maximum of the $Re(Z_{in})$ with respect to f_S, i.e.,

$$f_{max(Re)} = \sqrt{\frac{2Q^2}{2Q^2-1}} \times f_S \approx \left(1+\frac{1}{4Q^2}\right) f_S \quad (14)$$

According to the above results, the frequency where the phase is minimal is coupling dependently, thus the accuracy obtained by measuring $f_{phase-dip}$ is decreased if k is not constant. Therefore, $Re(Z_{in})$ is preferred in applications where the distance or the alignment of the readout coil relative to the LC-type sensor cannot be maintained.

B. Readout Circuit

In order to achieve a low-cost, portable telemetry unit for LC-type passive wireless sensors and also to avoid the coupling coefficient compensation, a SWR bridge (broadband diode detection) based readout prototype is implemented to extract the resonant frequency of the LC-type sensor. The proposed portable telemetry unit can sweep over the specific frequency range (not exceed 60 MHz) and measure the real part of the readout coil impedance.

The telemetry circuit mainly consists of a micro controller module, a direct digital synthesizer (DDS) module, a bridge detector circuit module and a USB communication module,

as shown in Fig. 6(a). A brief description of the basic principles is presented below. The excitation signal is generated with a commercial DDS chip (AD9851). After filtering and amplification, the signal is fed to the detector circuit. Then, the circuit measures four scalar voltages of the SWR bridge for impedance calculations.

The micro controller is used to implement three functions: controlling the DDS module, digitizing the above four voltages by using internal fast 12-bit ADCs, and communicating with a laptop PC via a USB port. At this stage of the readout system, the PC is used to input the sweep parameters (start frequency, end frequency, and frequency step) and also to post process the measured data. The implements in hardware and software of the above functions are well-known in normal frequency-sweep circuit, so we will focus on the detector module.

The used detector circuit is basically a SWR bridge with four envelope diodes, as shown in Fig. 6(b). The SWR bridge is actually an imbalance Wheatstone bridge, which consists of three known legs (50Ω resistors) and a readout coil as the left unknown leg. Four voltages are measured such as the incident RF source voltage (V_I), the unbalanced bridge voltage (V_R), the voltage at the readout coil (V_Z), and the voltage across the known resistance of the leg of the load (V_S). The internal ADCs of micro controllers are used to convert these four analog voltages to digital ones. Then, $Re\,(Z_{in})$ can be calculated from these four voltages as following formulas.

First, the imbalance voltage V_R can be expressed as

$$V_R = \left(\frac{Z_{in}}{Z_{in}+50} - \frac{1}{2}\right) V_I \tag{15}$$

The reflection coefficient ρ at the terminal of the readout coil is

$$\rho = \frac{Z_{in}-50}{Z_{in}+50} \tag{16}$$

From equation (15) and (16), ρ can be expressed as

$$\rho = V_R \Big/ \frac{V_I}{2} \tag{17}$$

Thus, standing wave ratio is

$$\mathrm{SWR} = \frac{1+|\rho|}{1-|\rho|} = \frac{\left|\frac{1}{2}V_I\right| + |V_R|}{\left|\frac{1}{2}V_I\right| - |V_R|} \tag{18}$$

Magnitude of Z_{in} can be easily get as

$$|Z_{in}| = \frac{50 \times V_Z}{V_s} \tag{19}$$

Now, we can get from SWR and $|Z_{in}|$ by solving the follow equation

$$\frac{|Z_{in}|^2 + 50^2 - 100Re\,(Z_{in})}{|Z_{in}|^2 + 50^2 + 100Re\,(Z_{in})} = \left(\frac{SWR-1}{SWR+1}\right)^2 \tag{20}$$

Thus, $Re\,(Z_{in})$ can be expressed as

$$Re\,(Z_{in}) = \frac{\left(|Z_{in}|^2 + 50^2\right) \times SWR}{50 \times \left(SWR^2+1\right)} \tag{21}$$

The software in the microcontroller calculates the input impedance real part by using the above Eqs. (18), (19) and (21) from four digitized voltages at each sweep frequency. At last, PC post-processing software plots $Re\,(Z_{in})$ curve versus frequency and finds the peak frequency.

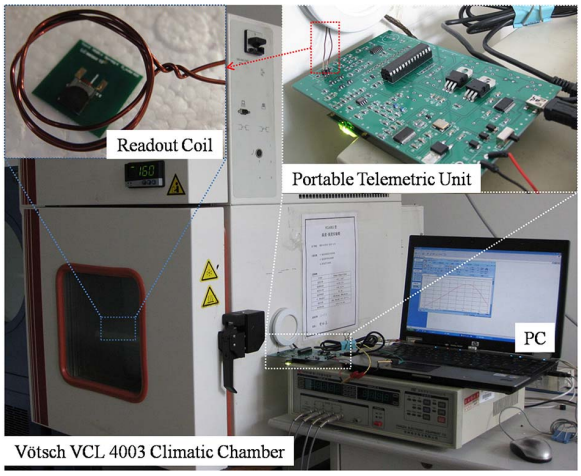

Fig. 7. Humidity measurement setup with the homemade readout circuit.

IV. Setup and Results

The LC-type passive wireless graphene oxide based humidity sensor is tested in a climate chamber. The humidity-testing setup is shown in Fig. 7. A manually wound external readout coil (24 AWG copper wire, 3 turns and 15 mm diameter) is connected to the external telemetry circuit and is collinearly placed with the sensor in the chamber at a distance of about 5 mm.

For humidity response, RH of the chamber was raised from 15% to 95% with a step of 10% and the temperature was maintained at 25°C. The interval time of the adjacent test point was 40 min to improve the veracity of measurement. After every group of measurements, the sensor was placed in drying oven for 1 hour. More than 10 groups of measurements were performed and the results show a good repeatability.

Fig. 8 shows the measured $Re\,(Z_{in})$ as a function of the frequency for different humidity levels at 25°C. The measured resonant frequency (at 10kHz, 25°C, and 55%RH) is about 36.2MHz, which is lower than the calculated one (5.8% error), as shown in Table I. This is probably due to fact that interconnection between the inner and outer end of the inductor and bonding wires are not taken into account. The error is acceptable for the aim to confine the resonant frequency of the sensor tank to locate in proper frequency band of our custom-made readout circuit through pre-computation.

As the humidity increases, the maximum real part of the impedance shifts monotonically to lower frequencies because the interdigital capacitance increases. This variation trend of the capacitance with humidity is totally contrary to the previous work [17]. The explanation is that the frequency-dependent relative dielectric constant of graphene oxide drops below that of water in the operating frequency range (30-40 MHz) [24]. The maximum $Re\,(Z_{in})$ magnitude becomes smaller as the resonant frequency decreases, which can be explained by the reduction of the quality factor of the LC-type sensor tank as the capacitance increases. The sensitivity of the LC-type passive wireless humidity sensor based on graphene oxide is about −18.75 kHz/%RH.

For comparison, an LC-type passive wireless sensor with polyimide as sensing material is also characterized and the

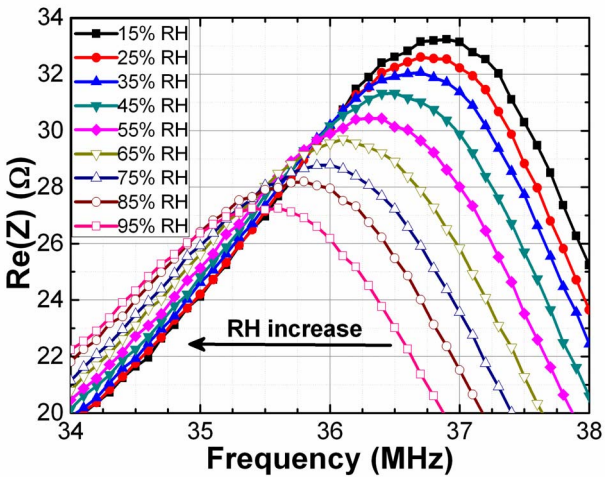

Fig. 8. Measured maximum $Re\,(Z_{in})$ frequency shift as a function of humidity at 25°C (graphene oxide).

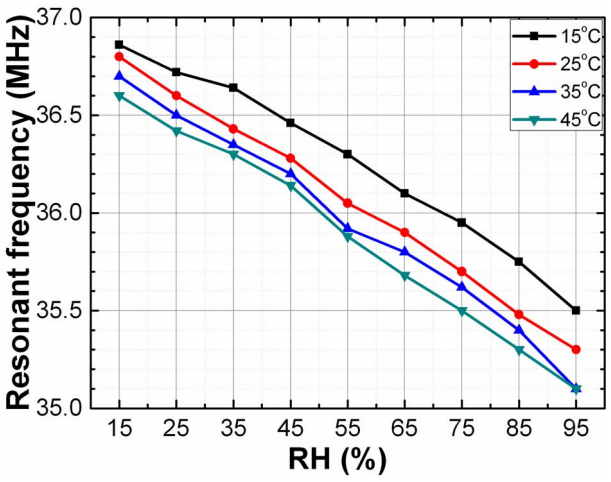

Fig. 10. Measured resonant frequency versus humidity at 15, 25, 35, or 45 °C.

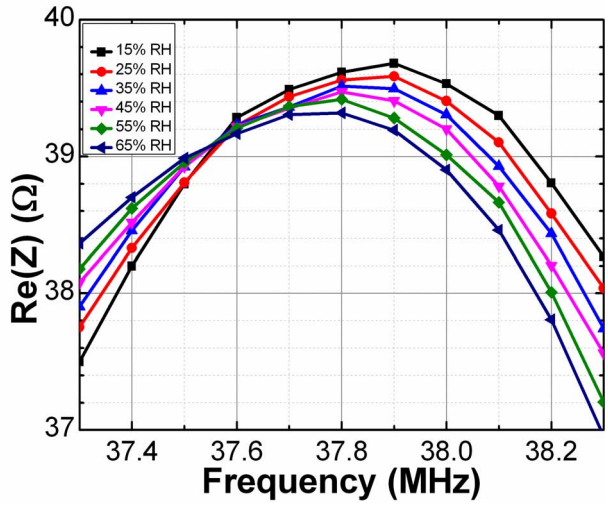

Fig. 9. Measured maximum $Re\,(Z_{in})$ frequency shift as a function of humidity at 25°C (polyimide).

measured result is shown in Fig. 9. The changes of the $Re\,(Z_{in})$ curves with different humidity levels are hardly to be distinguished and the sensitivity is only about −2.4kHz/RH%. It is worth reminding that the used CMOS capacitive sensors have polysilicon heaters. The parasitic capacitance is increased significantly due to the existence of these heaters. When used as wired sensor, the heaters and substrate are both grounded to suppress the parasitic capacitance. However, these heaters are floating when used as LC-type passive wireless sensor, thus the floating capacitance is connected with inductor. So, the sensitivity of sensors with both GO or polyimide can be improved without the heaters.

Fig. 10 presents the relationship between the measured resonant frequency of the sensor based on graphene oxide films with relative humidity at different temperatures (15°C, 25°C, 35°C, 45°C). It is clear from the results that the resonant frequency decreases as the temperature increase and the temperature dependence is about −13kHz. However, the humidity sensitivity slightly varies at different temperatures. Actually, graphene oxide can be exploited in both humidity and temperature sensors. Future work will be focused on decoupling the humidity and temperature responses for practical applications. From Fig. 10, it can be concluded that the sensitivity slightly varies at different temperatures.

V. Conclusion

This paper presents an LC-type passive wireless humidity sensor based on graphene oxide and its associated portable telemetry unit. The sensor consists of a CMOS interdigital capacitive humidity-sensitive sensor die and a fixed planar spiral copper inductor on a FR-4 substrate, forming a resonant LC tank circuit. By using graphene oxide as sensing material the sensitivity of the LC-type sensor is improved significantly. The package-level integration is achieved by employing the embedded inductors on organic packaging substrates. The sensor is wirelessly interrogated by using our customized portable telemetry unit. The proposed reader is based on a SWR bridge and measures the real part of the readout coil impedance. This telemetry unit addresses the need for a low-cost, portable reader and is also suitable for other LC-type passive wireless sensors. Experimental results show a sensitivity of −18.75 kHz/%RH over a range of 15-95% RH.

References

[1] M. A. Fonseca, J. M. English, M. von Arx, and M. G. Allen, "Wireless micromachined ceramic pressure sensor for high-temperature applications," *J. Microelectromech. Syst.*, vol. 11, no. 4, pp. 337–343, Aug. 2002.

[2] A. Baldi, W. Choi, and B. Ziaie, "A self-resonant frequency-modulated micromachined passive pressure transensor," *IEEE Sensors J.*, vol. 3, no. 6, pp. 728–733, Dec. 2003.

[3] N. Xue, S.-P. Chang, and J.-B. Lee, "A SU-8-based microfabricated implantable inductively coupled passive RF wireless intraocular pressure sensor," *J. Microelectromech. Syst.*, vol. 21, no. 6, pp. 1338–1346, Dec. 2012.

[4] Y. Jia, K. Sun, F. J. Agosto, and M. T. Quiñones, "Design and characterization of a passive wireless strain sensor," *Meas. Sci. Technol.*, vol. 17, no. 11, pp. 2869–2876, Nov. 2006.

[5] Y. Wang, Y. Jia, Q. Chen, and Y. Wang, "A passive wireless temperature sensor for harsh environment application," *Sensors*, vol. 8, no. 12, pp. 7982–7995, 2008.

[6] J.-C. Kuo, P.-H. Kuo, Y.-T. Lai, C.-W. Ma, S.-S. Lu, and Y.-J. J. Yang, "A passive inertial switch using MWCNT–hydrogel composite with wireless interrogation capability," *J. Microelectromech. Syst.*, vol. 22, no. 3, pp. 646–654, Jun. 2013.
[7] S. Bhadra, D. S. Y. Tan, D. J. Thomson, M. S. Freund, and G. E. Bridges, "A wireless passive sensor for temperature compensated remote pH monitoring," *IEEE Sensors J.*, vol. 13, no. 6, pp. 2428–2436, Jun. 2013.
[8] P.-J. Chen, D. C. Rodger, S. Saati, M. S. Humayun, and Y.-C. Tai, "Microfabricated implantable parylene-based wireless passive intraocular pressure sensors," *J. Microelectromech. Syst.*, vol. 17, no. 6, pp. 1342–1351, Dec. 2008.
[9] G. Jacquemod, M. Nowak, E. Colinet, N. Delorme, and F. Conseil, "Novel architecture and algorithm for remote interrogation of battery-free sensors," *Sens. Actuators A, Phys.*, vol. 160, nos. 1–2, pp. 125–131, May 2010.
[10] O. Akar, T. Akin, and K. Najafi, "A wireless batch sealed absolute capacitive pressure sensor," *Sens. Actuators A, Phys.*, vol. 95, no. 1, pp. 29–38, Dec. 2001.
[11] E. Sardini and M. Serpelloni, "Wireless measurement electronics for passive temperature sensor," *IEEE Trans. Instrum. Meas.*, vol. 61, no. 9, pp. 2354–2361, Sep. 2012.
[12] T. Salpavaara, J. Verho, P. Kumpulainen, and J. Lekkala, "Readout methods for an inductively coupled resonance sensor used in pressure garment application," *Sens. Actuators A, Phys.*, vol. 172, no. 1, pp. 109–116, Dec. 2011.
[13] Y. Y. Qiu, C. Azeredo-Leme, L. R. Alcácer, and J. E. Franca, "A CMOS humidity sensor with on-chip calibration," *Sens. Actuators A, Phys.*, vol. 92, nos. 1–3, pp. 80–87, Aug. 2001.
[14] L. Gu, Q.-A. Huang, and M. Qin, "A novel capacitive-type humidity sensor using CMOS fabrication technology," *Sens. Actuators B, Chem.*, vol. 99, nos. 2–3, pp. 491–498, May 2004.
[15] L.-T. Chen, C.-Y. Lee, and W.-H. Cheng, "MEMS-based humidity sensor with integrated temperature compensation mechanism," *Sens. Actuators A, Phys.*, vol. 147, no. 2, pp. 522–528, Oct. 2008.
[16] T. J. Harpster, S. Hauvespre, M. R. Dokmeci, and K. Najafi, "A passive humidity monitoring system for *in situ* remote wireless testing of micropackages," *J. Microelectromech. Syst.*, vol. 11, no. 1, pp. 61–67, Feb. 2002.
[17] C.-L. Zhao, M. Qin, W.-H. Li, and Q.-A. Huang, "Enhanced performance of a CMOS interdigital capacitive humidity sensor by graphene oxide," in *Proc. 16th Int. Solid-State Sens., Actuators, Microsyst. Conf. (TRANSDUCERS)*, Beijing, China, Jun. 2011, pp. 1954–1957.
[18] S. S. Mohan, M. D. M. Hershenson, S. P. Boyd, and T. H. Lee, "Simple accurate expressions for planar spiral inductances," *IEEE J. Solid-State Circuits*, vol. 34, no. 10, pp. 1419–1424, Oct. 1999.
[19] C.-L. Zhao, M. Qin, and Q.-A. Huang, "A fully packaged CMOS interdigital capacitive humidity sensor with polysilicon heaters," *IEEE Sensors J.*, vol. 11, no. 11, pp. 2986–2992, Nov. 2011.
[20] C. Zhang, J. Q. Huang, and Q. A. Huang, "A passive wireless graphene oxide based humidity sensor and associated portable telemetry unit," in *Proc. 17th Int. Conf. Solid-State Sens., Actuators, Microsyst. (TRANSDUCERS EUROSENSORS)*, Barcelona, Spain, Jun. 2013, pp. 278–181.
[21] S. Sauer, U. Marschner, B. Adolphi, B. Clasbrummel, and W. Fischer, "Passive wireless resonant galfenol sensor for osteosynthesis plate bending measurement," *IEEE Sensors J.*, vol. 12, no. 5, pp. 1226–1233, May 2012.
[22] J. Joy, J. Kroh, M. Ellis, M. Allen, and W. Pyle, "Communicating with implanted wireless sensor," U.S. Patent 7 245 117, Jul. 17, 2007.
[23] R. Nopper, R. Niekrawietz, and L. Reindl, "Wireless readout of passive *LC* sensors," *IEEE Trans. Instrum. Meas.*, vol. 59, no. 9, pp. 2450–2457, Sep. 2010.
[24] D. W. Lee *et al.*, "Transparent and flexible polymerized graphite oxide thin film with frequency-dependent dielectric constant," *Appl. Phys. Lett.*, vol. 95, no. 17, pp. 172901-1–172901-3, Oct. 2009.

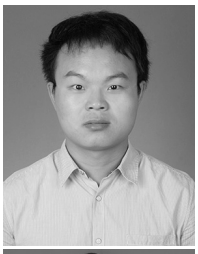

Cong Zhang received the B.S. degree in electronic engineering from Southeast University, Nanjing, China, in 2009, where he is currently pursuing the Ph.D. degree with the Key Laboratory of MEMS, Ministry of Education.

His research interests include humidity sensors, MEMS inductors, wireless passive microsensor, and inductive telemetry technique.

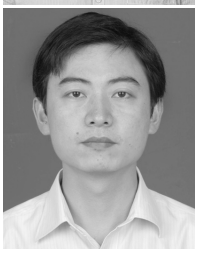

Li-Feng Wang (M'13) was born in China in 1981. He received the B.S., M.S., and Ph.D. degrees in electrical engineering from Southeast University, Nanjing, China, in 2003, 2006, and 2013, respectively. From 2006 to 2008, he was with the Nanjing Electronic Device Institute, where he worked on silicon micromechanical devices.

He joined the faculty of the Department of Electronic Engineering, Southeast University, as an Assistant Professor. His current research interests include the design, fabrication, and reliability of wireless microsensors and micromachined RF/MW switches.

Jian-Qiu Huang (M'11) was born in China in 1981. He received the B.S., M.S., and Ph.D. degrees in electrical engineering from Southeast University, Nanjing, China, in 2004, 2007, and 2011, respectively.

He joined the faculty of the Department of Electronic Engineering, Southeast University, as an Assistant Professor. His main research interests are CMOS-MEMS technology, MEMS humidity sensors, and MEMS temperature sensors.

Qing-An Huang (S'89–M'91–SM'95) received the B.S. degree from the Hefei University of Technology, Hefei, China, in 1983; the M.S. degree from Xidian University, Xi'an, China, in 1987; and the Ph.D. degree from Southeast University, Nanjing, China, in 1991, all in electronic engineering. His Ph.D. research focused on micromachined GaAs piezoelectric sensors.

He joined the faculty of the Department of Electronic Engineering, Southeast University, after graduation, where he became a Full Professor in 1996, and was appointed to Chair Professor of the Chang-Jiang Scholar by the Ministry of Education in 2004. He is currently the Founding Director of the Key Laboratory of MEMS, Ministry of Education, Southeast University. He has authored a book entitled *Silicon Micromachining Technology* (Science Press, 1996), has published over 150 peer-reviewed international journals/conference papers, and holds 40 Chinese patents.

Dr. Huang is currently serving as an Editor-in-Chief of the *Chinese Journal of Sensors and Actuators*, and an Editorial Board Member of the *Journal of Micromechanics and Microengineering*. He was the Conference Co-Chair of the *SPIE-Microfabrication and Micromachining Process Technology and Devices* (Proc.SPIE, vol.4601, 2001), the TPC Co-Chair of the 7th IEEE International Conference on Nano/Micro Engineered and Molecular System (NEMS) (Kyoto, 2012), the 6th Asia-Pacific Conference of Transducers and Micro/Nano Technologies (Nanjing, 2012), the TPC Member of Transducers from 2009 to 2013, and the IEEE Sensors Conference from 2002 to 2013. He has served as the Founding Chairman of the IEEE Electron Devices (ED)-Solid-State Circuits (SSC) Nanjing Chapter. He was a recipient of the National Outstanding Youth Science Foundation Award of China in 2003.